Available online at www.sciencedirect.com
ScienceDirect
Trans. Nonferrous Met. Soc. China 23(2013) 1949−1956
Transactions of Nonferrous Metals Society of China
www.tnmsc.cn

Fatigue behavior of friction stir spot welded AZ31 Mg alloy sheet joints

Tian-jiao LUO, Bao-liang SHI, Qi-qiang DUAN, Jun-wei FU, Yuan-sheng YANG

Institute of Metal Research, Chinese Academy of Sciences, Shenyang 110016, China

Received 11 June 2012; accepted 10 December 2012

Abstract: The fatigue behavior of friction stir spot welded (FSSW) AZ31 magnesium alloy sheet joints was investigated by tension−compression of fatigue test. The results suggest that all the fatigue failures occur at the stir zone of the FSSW AZ31 sheet joints, and all cracks initiate at the stir zone outer edge between the upper and lower sheet. When the cycle force equals 1 kN, the crack propagates along the interface of heat-affected zone and thermo-mechanical zone, simultaneously across the direction of force; while the cycle force equals 3 kN, the crack propagates along the diameter of stir zone and shear failure occurs finally. Moreover, the transverse microsections indicate that there is a tongue-like region at the outer edge of stir zone between the two AZ31 sheets, and the direction of tongue-like region is toward outside of the stirred zone and all fatigue cracks initiate at the tongue-like region.

Key words: AZ31 Mg alloy sheet; friction stir spot welding; fatigue; fatigue failure; fatigue crack

1 Introduction

Recently, the automobile industry has been facing a critical challenge to lower the weight of automobile which not only can reduce the gasoline consumption, but also can lower the cost of automobile manufacturing, which enhances the interest in the study of lightweight materials for structural components [1,2]. Magnesium alloys have lower density, higher specific strength and better workability, which have absorbed the attention of researchers and automobile designers, and developed countries attach great importance to magnesium alloys in the transport application such as automobile [3,4]. For the importance of joining of structures made of magnesium alloys, recently, the welding methods of magnesium alloys including laser welding, arc-welding, friction stir welding (FSW) and so on have been developed. Among them the FSW is regarded as the most significant development in metal joining in a decade, and FSW has some merits, such as high retention of bulk mechanical properties, low distortion, low residual stresses and low defects joining technology, which is applied in the fields of aerospace industry and transportation industry extensively [5−7]. The friction stir spot welding (FSSW), a variant of FSW, has the same merits as the FSW technology, so it is expected to be applied to the joining of structure components extensively. For magnesium alloys, most of studies about the FSSW are concentrated on the welding process [8−10]. YIN et al [8] evaluated the effects of the tool geometry and dwell time settings on the microstructure features and mechanical properties of AM60 and AZ31 FSSW joints. YAMAMOTO et al [9] investigated the liquid penetration induced cracking tendencies during AZ91, AZ31 and AM60 FSSW. It was found that cracking occurred early in the dwell period in AZ91, AZ31 and AM60 FSSW and crack-free FSSW joints were produced when the dwell time is more than 4 s. YANG et al [10] developed a new model of material flow during FSSW on the basis of experimental observations, and believed that the intrinsic driving force for the downward motion of the plasticized material was originated from the material release from the rotating pin through an outward-spinning motion. However, when the FSSW was applied to the joining of load-carrying construction, the strength, especially the fatigue properties of the load-carrying construction become critical, the fatigue behavior of the FSSW joint should be researched systematically, and the fatigue properties must be evaluated to ensure the integrity and security of the joint, which benefit the designers to select good

Foundation item: Project (2007CB613705) supported by the National Key Technologies R&D Program of China; Project (2011DFA50902) supported by the International S&T Cooperation Program of China
Corresponding author: Yuan-sheng YANG; Tel: +86-24-23971728; Fax: +86-24-23844528; E-mail: ysyang@imr.ac.cn
DOI: 10.1016/S1003-6326(13)62682-5

materials and good design scheme of load-carrying construction. Recently, some studies have been carried out to investigate the mechanical and fatigue properties of FSSW magnesium alloys [11−13]. YIN et al [11] argued the hook formation and the overlap shear strength properties of AZ31 FSSW joints, and found that the failure load properties were highest in AZ31 FSSW welds made using a dwell time of 1 s and were decreased when the dwell period was further extended. YIN et al [12] also investigated the stir zone microstructures and mechanical properties of dissimilar AZ91/AZ31 FSSW welds, and believed that the distance from the tip of the hook region to the keyhole periphery was a dominant factor influencing the mechanical properties of dissimilar AZ91/AZ31 FSSW joints. In addition, LIN et al [13] demonstrated that tool rotational speed, plunge rate, and dwell time were varied to determine their effects on the microstructure, fracture behavior, and mechanical properties of welds. However, there was limited published literature about fatigue properties of the FSSW magnesium alloys [14,15]. MALLICK and AGARWAL [14] studied and discussed the fatigue behaviors of FSSW joints in lap shear specimens of AM60 magnesium alloy and AA 5754 aluminum alloy, and analyzed the stress distribution and the location of maximum stresses in FSSW joints in Mg−Mg specimens by finite element method. JORDAN et al [15] quantified the fatigue performance and failure mechanisms of FSSW in AZ31 alloy, and presented the modeling comparison with the experimental results.

In the present work, the fatigue behavior of FSSW specimens was investigated for AZ31 magnesium alloy sheet, the fatigue strength and fatigue crack propagation characteristic were discussed in detail, and the fatigue failure mechanism of FSSW AZ31 alloy sheet joints was also represented profoundly.

2 Experimental

2.1 Material

In this investigation, AZ31 magnesium alloy sheets with a thickness of 2 mm were used. The chemical composition of AZ31 magnesium alloy sheets is listed in Table 1. Figure 1(a) shows the microstructure of the rolled AZ31 magnesium alloy sheet observed in three planes by scanning electron microscopy (SEM) analyses, which indicates that there are some deformation bands across the rolling direction (RD) in normal direction (ND) planes. In the section along RD direction, there are also some deformation bands which have 45° to RD direction. There are some equiaxed grains and elongated grains in the section along RD direction. In the section along transverse direction (TD), the direction of the deformation bands is parallel to TD direction, and there are also many finer equiaxed grains. During rolling process, AZ31 alloy sheet is compressed along the ND direction and pulled along the RD direction, which results in the formation of above microstructures, namely, polycrystal structures with preferred orientation. Figure 1(b) shows the texture of AZ31 sheet gained by XRD technology. It can be seen that there is a strong basal texture in the sheet, with a maximum intensity of 21.89. The mentioned-above microstructure characteristic of AZ31 alloy sheet will affect the properties of FSSW AZ31 alloy sheet joint significantly.

Table 1 Chemical composition of AZ31 magnesium alloy sheets (mass fraction, %)

Al	Zn	Mn	Si	Cu
2.95	0.97	0.42	0.1	0.05

Ni	Fe	Ca	Mg
0.005	0.005	0.04	Bal.

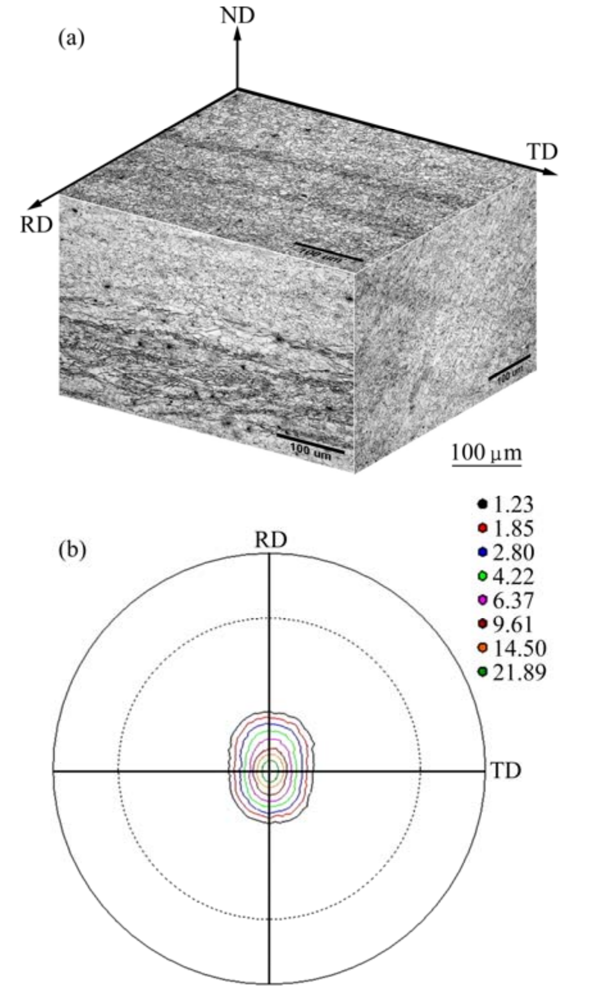

Fig. 1 Microstructure of rolled AZ31 sheet: (a) Microstructure observed in three planes; (b) {0002} pole figure of rolled sheet

2.2 Specimens

Coupons for single lap joint welds (Fig. 2) will be used to evaluate the fatigue behavior of sheet Mg AZ31 alloy. The specimens with total length of 162 mm and width of 38 mm were machined in the rolling direction, and the length of the lap section was 38 mm. In order to prevent additional bending forces, Mg AZ31 shims of 2 mm in thickness and 26 mm in length were employed during fatigue tests.

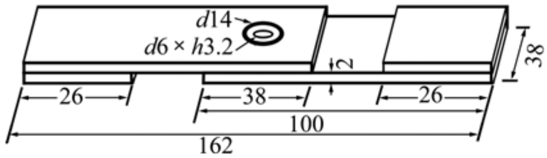

Fig. 2 Test specimen for fatigue test (unit: mm)

The diameter of rotating tool position was 14 mm, the diameter of the pin position was 8 mm and the depth of FSSW pole was 3.2 mm.

2.3 Procedures

Fatigue tests were conducted using a completely computer-controlled Instron 8871 servo-hydraulic testing system under force control at different force amplitudes, with 70 bar of chucking power. At each force level at least two samples were tested. For the fatigue tests proposed, coupons were to be run at the force ratio of R (F_{min}/F_{max}) equals 0.1, the tests were conducted at a frequency of 5 Hz and at two F_{max} force levels: 1 kN and 3 kN. Sinusoidal waveform was selected in all the tests. During the fatigue testing, shims were used to maintain co-planar alignment (Fig. 2).

The piece used to examine the cross-sectional microstructure of FSSW section was cut in the direction along the welding point, and the piece was cold mounted with epoxy resin, then the specimen was ground, polished and etched. The etchant employed during this investigation comprised 4.2 g picric acid, 10 mL acetic acid (99%), 10 mL H_2O and 70 mL ethanol (95%).

After the fatigue tests the base metal and the FSSW position were examined by SEM (JSM-6301F) equipped with energy dispersed spectroscopy (EDS) system.

3 Results and discussion

3.1 Microstructure and tensile performance

The macro-photograph of the transverse section through the center of the FSSW joint and the microstructures of different zones at the FSSW joint of AZ31 sheets are shown in Fig. 3. Figure 3(a) shows the macroscopic structure of the transverse section of the FSSW joint, where the heat-affected zone, thermo-mechanical zone and stirred zone can be seen. The macrostructure of the transverse section suggests that the upper sheet connect tightly with the lower sheet by the FSSW technology, and the microstructure of welding zone is different from that of the base metal (Fig. 1(b)). In the rolled sheet, there are some deformation bands, and there is a strong basal texture in the sheet with a maximum intensity of 21.89. However, more or less recrystallization occurs in the welding zone (shown in Figs. 3(b)−(e)). According to MISHRA and MA [6], the FSW process can be modeled as a metal working process, when the rotating tool contacts the upper sheet and a downward force is applied, the friction heat is generated, then the heated AZ31 alloy softens and deforms plastically, which results in more or less dynamic recrystallization, forming a number of different size equiaxed grains. Compared with other zones of the FSSW joint, the number of equiaxed grain in the stirred zone is significantly more and the size is smaller. Figure 4 shows the typical hardness of different zones. The results indicate that the hardness values of stirred zone is higher than those of base metal, which suggests that softening not occurs in AZ31 alloy sheet during the FSSW process. The increment in hardness is mainly correlated with the grain refinement and the precipitate distribution, as shown in Figs. 3(b)−(e), some equiaxed-shape precipitates of less than or equal to 5 μm in diameter are observed in the heat-affected zone, thermo-mechanical zone and stirred zone. This result is different from that reported in Refs. [16−18], which is perhaps caused by the strain-softening and grain growth in the welding zone during the FSW process, especially in stirred zone.

3.2 Fatigue life of FSSW AZ31 sheet joints

Force controlled fatigue tests were conducted on the FSSW specimens, and the obtained results are shown in Fig. 5. It can be seen that the fatigue life of coupons at 1 kN is longer than 1×10^5 cycles, but the fatigue properties of AZ31 FSSW coupons are unstable under the force of 1 kN; the fatigue life of coupons at 3 kN is longer than 1×10^4 cycles, the fatigue properties of AZ31 FSSW coupons are stable comparatively under the force of 3 kN, and the fatigue life of coupons at 3 kN is longer than 1×10^4 cycles. In addition, all the specimens at higher maximum force have a lower fatigue life than that at lower maximum force.

Figure 6 shows the maximum relative displacement under the different force amplitude of 1 kN and 3 kN. It suggests that the maximum relative displacement under the force of 3 kN increases significantly when the number of cycles increases, which indicates that the cyclic softening occurs remarkably under the force of 3 kN. However, the maximum relative displacements of

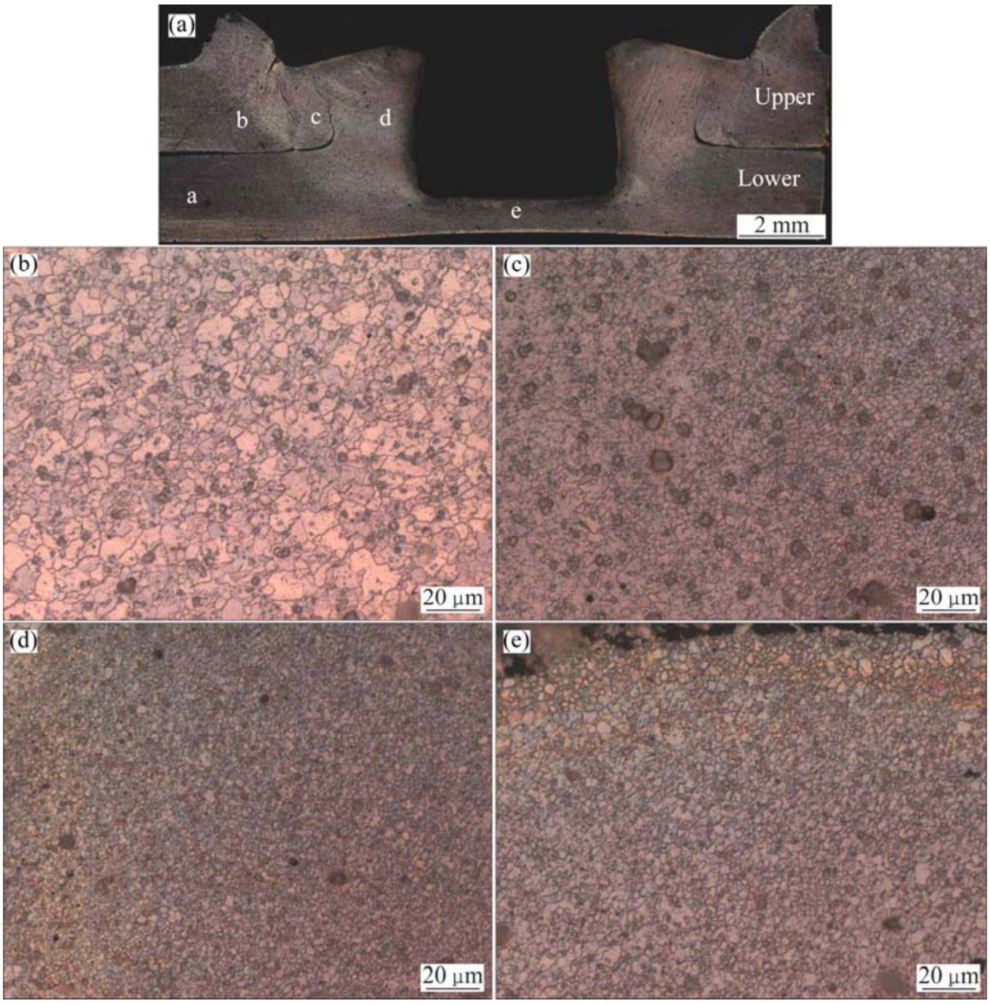

Fig. 3 Macroscopic structure of transverse section through center of FSSW joint and microstructures of different zone at FSSW joint of AZ31 sheets: (a) Macroscopic structure of transverse section of FSSW joint (a—Base metal; b—Heat-affected zone; c—Thermo-mechanical zone; d—Stirred zone; e—Stirred zone below); (b) Microstructure of heat-affected zone; (c) Microstructure of thermo-mechanical zone; (d) Microstructure of stirred zone; (e) Microstructure of stirred zone below

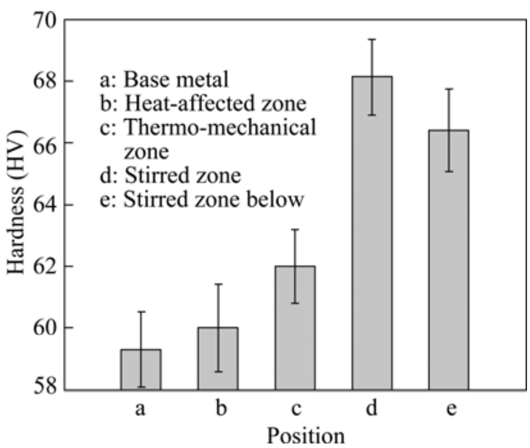

Fig. 4 Typical hardness of different zones

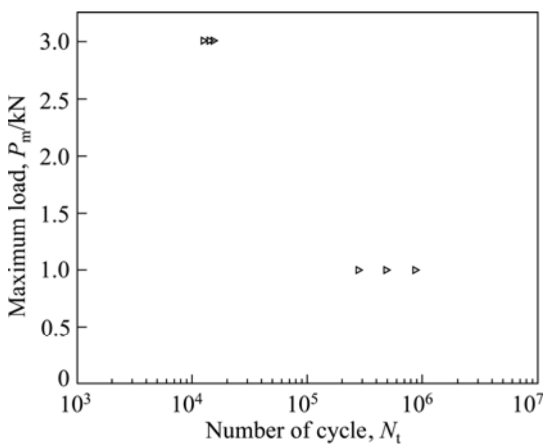

Fig. 5 Fatigue life of FSSW AZ31 sheet joints

different cycles under the force of 1 kN are basically the same, the cyclic softening or cyclic hardening does not generate under the force of 1 kN. According to the cyclic deformation mechanism of ductile metal [19], under the cyclic force, for the ductile metal cyclic softening occurs for its work-hardening before and the rearrangement of the introduced dislocation network because of the pre-strain. The reason of the cyclic softening under the force

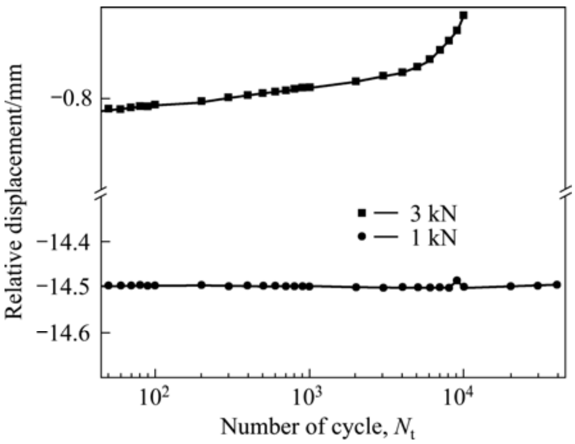

Fig. 6 Maximum relative displacement of force amplitude with 1 kN and 3 kN

of 3 kN is probably because the work-hardening occurs in the welding zone during the FSSW process, and when the AZ31 FSSW joint specimen is imposed with the cyclic force of 3kN, the dislocation network rearranges.

3.3 Analysis of fatigue fracture

During the test all the fatigue failure occurred at the stir zone of the FSSW AZ31 magnesium alloy sheet joints. The fatigue fractures and the crack propagation area characteristics of FSSW AZ31 magnesium alloy sheet joints are shown in Fig. 7. It can be found that all cracks initiate at the stir zone outer edge between the upper sheet and lower sheet. However, the failure mode at the lower force level of 1 kN is different from that at higher force level of 3 kN. When the cyclic force is equal to 1 kN, the crack propagates along the interface of the heat-affected zone and the thermo-mechanical zone, simultaneously across the direction of force (Fig. 7(a)). Probably because the strength of the interface region of the heat-affected zone and the thermo-mechanical zone is relatively smaller (Fig. 4) or some residual stresses are distributed in the interface zone, the micro-crack is easier to form and propagate along the interface of the heat-affected zone and the thermo-mechanical zone. When the cyclic force is equal to 3 kN, the crack propagates along the diameter of stir zone and shear failure occurs finally (Fig. 7(c)). In order to prevent additional bending forces, Mg AZ31 shims of 2 mm in thickness are employed as shown in Fig. 2, however, because the upper sheet is not at the same plane with the lower sheet, there are bending forces acting on the joint of the two sheets during the cyclic tension process, which make it possible that all cracks initiate at the stir zone outer edge between the upper sheet and lower sheet.

Moreover, SEM images of the coupons show that some striation-like features are observed in the crack propagation area (As shown in Figs. 7(b) and (d)), and the striations are perpendicular to the crack propagation direction. Similar to the explanation of the idealized plastic passivation model for the formation of fatigue striation and the second-stage of the fatigue crack

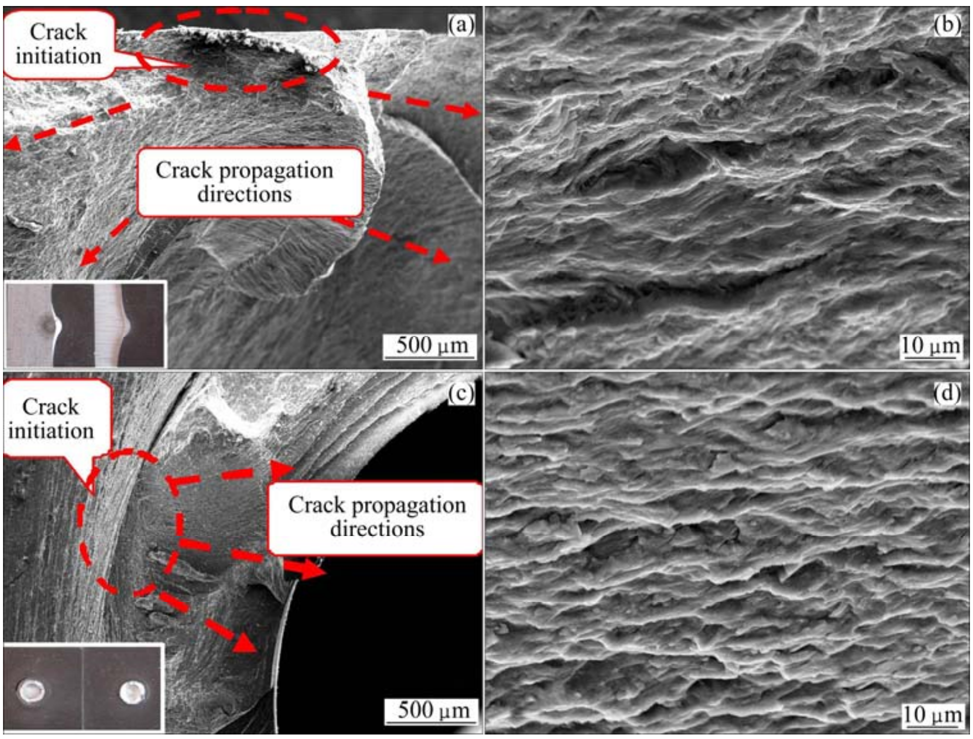

Fig. 7 Fatigue fractures and crack propagation area characteristics of FSSW AZ31 magnesium alloy sheet joints: (a), (b) 1 kN; (c), (d) 3 kN

propagation presented by LAIRD [20], it is believed that the fatigue crack propagates forward some distance in each force cycle, which is induced by the plasticity passivation of crack tip. When the cyclic force is greater than $(F_{max}+F_{min})/2$, the plastic passivation occurs at the crack tip for the duplex slip, which makes the crack extend forward some distance. If the far-field cyclic force is less than $(F_{max}+F_{min})/2$, the crack tip will be re-sharpening, however, which can not completely eliminate the effect of passivation caused by the cyclic force greater than $(F_{max}+F_{min})/2$, therefore, under the cyclic force greater than $(F_{max}+F_{min})/2$, the crack will propagate forward some distance again, which leads to the formation of the fatigue striation.

3.4 Fatigue failure mechanism of FSSW AZ31 alloy sheet joints

Figure 8 shows the fatigue failure mechanism of FSSW AZ31 alloy sheet joints. Figures 8(a) and (b) indicate that there is a tongue-like region at the outer edge of the stir zone between the two AZ31 sheets, and the direction of the tongue-like region is toward outside of the stirred zone. Because of the oxide layer or antioxidation coating on the surface of sheet, the magnesium alloy in the metallurgical joining zone can't bond together closely, which is different from the analysis by YIN et al [8,11]. They considered that the FSSW joints contain hook regions which direction is toward inside of the stirred zone. Under the action of cyclic force F (Fig. 8(c)), the cracks, Crack 1 and Crack 2 as shown in Fig. 8(d), initiate at different location of the stirred zone, then propagate along different directions. The failure direction at 1 kN is along Crack 1, and the crack propagates along the interface of heat-affected zone and thermo-mechanical zone, simultaneously across the direction of force (Fig. 8(e)); while the failure direction at 3 kN is along Crack 2, and the crack propagates along the diameter of stir zone and shear failure occur finally (Fig. 8(f)).

By analysing the forces on the FSSW joint, it can be considered that the cyclic force F acts on Crack 1 and crack 2 individually and the cyclic force F can be resolved into two components, a bending force perpendicular to the crack direction, and a shear force along the crack propagation direction, as shown in Fig. 9. For Crack 1, the cyclic force F can be resolved into F_1 and F_2, and the cyclic force F makes an angle θ_1 with F_1. Also, for Crack 2, the cyclic force F can be resolved into F_3 and F_4, and the cyclic force F makes an angle θ_2 with F_3.

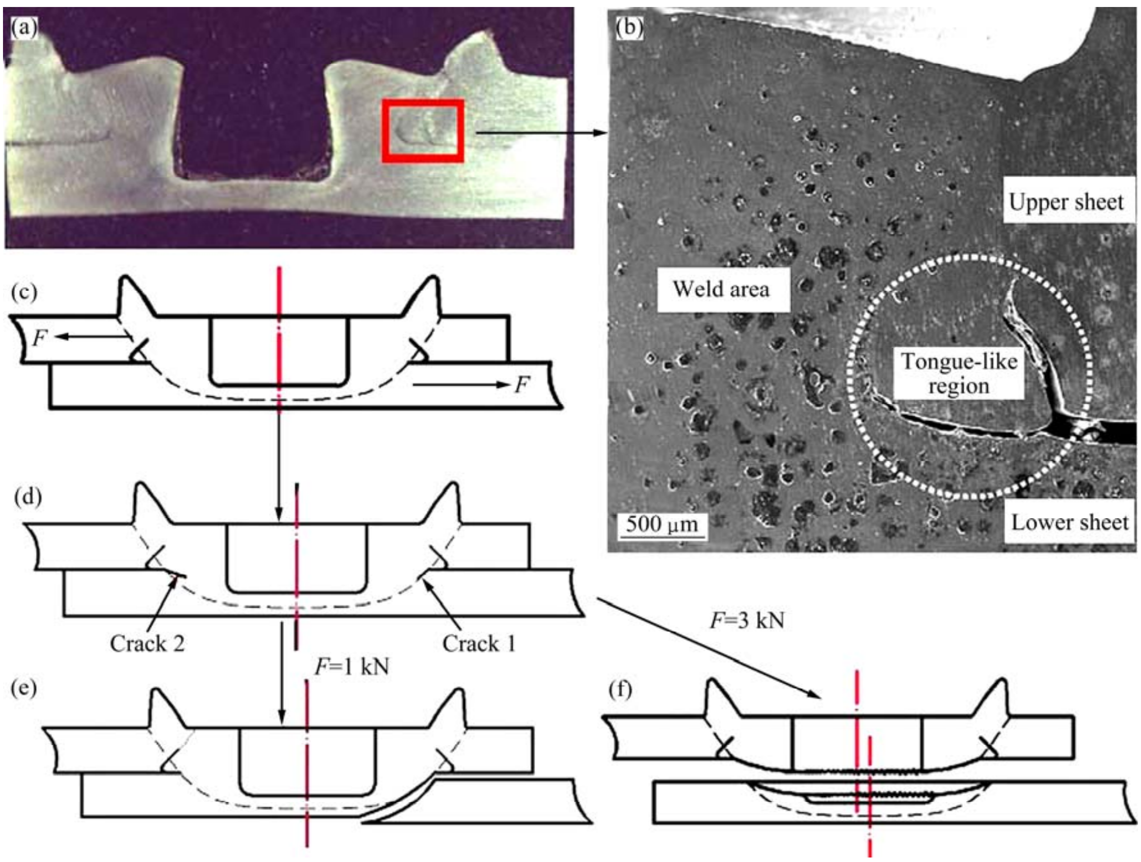

Fig. 8 Fatigue failure mechanism of FSSW AZ31 alloy sheet joints: (a) Macro-photograph of transverse section through center of FSSW joint; (b) Microstructure of stirred zone; (c) Before fatigue test; (d) Primary stage of crack propagation; (e) failure mode when F=1 kN; (f) Failure mode when F=3 kN

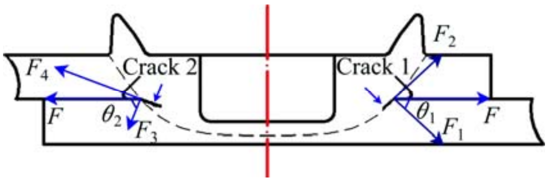

Fig. 9 Fracture mechanics analysis of FSSW joint under action of cyclic force

The bending forces, F_1 and F_3 are perpendicular to the crack direction, F_1 is equal to $F\cos\,\theta_1$, and F_3 is equal to $F\cos\,\theta_2$, the value of F_1 and F_3 will affect the propagation rate of the crack; F_2 and F_4 are the shear forces along the crack propagation direction, F_2 is equal to $F\sin\,\theta_1$, and F_4 is equal to $F\sin\,\theta_2$, F_2 and F_4 will make it possible that a shear fracture occurs at the stirred zone of the FSSW joint.

According to the fracture mechanics theory, the crack propagation rate is expressed as [21]

$$\upsilon = C(\Delta K)^m = C(Y\Delta\sigma\sqrt{\pi a})^m \quad (1)$$

where υ is the fatigue crack propagation rate; ΔK is the stress-intensity factor range; C, Y and m are constants that are functions of the material, environment, frequency, temperature, stress ratio, and geometric dimension; a is the crack length; $\Delta\sigma$ is the range of stress that is the algebraic difference between the maximum and minimum stress in a cycle, which is proportional to ΔF, the range of the bending force acting on the crack that is perpendicular to the crack direction.

For the Crack 1, ΔF is equal to ΔF_1, and ΔF_1= $0.9F\cos\,\theta_1$ (because the force ratio of R is equal to 0.1); similarly, for Crack 2, ΔF is equal to ΔF_3, ΔF_3= $0.9F\cos\,\theta_2$. Since $0°<\theta_1<\theta_2<90°$, ΔF_1 is bigger than ΔF_3, in addition, F_4 is bigger than F_2. Therefore, according to Eq. (1), it can be concluded that the fatigue crack propagation rate of Crack 1 is bigger than that of Crack 2, and normally, the fatigue fracture occurs along Crack 1, but when the F_4 is greater than the critical resolved shear force of the stirred zone, the shear fracture will take place along Crack 2. Therefore, when F=1 kN, F_4 is less than the critical resolved shear force of the stirred zone, the fatigue cracks propagate along the directions of Crack 1 and Crack 2, and finally the fatigue fracture occurs along Crack 1 (Fig. 7(a) and Fig. 8(e)); however, when F=3 kN, F_4 is greater than the critical resolved shear force of the stirred zone, the fatigue cracks also propagate along the directions of Crack 1 and Crack 2, but ultimately the shear fracture takes place.

4 Conclusions

1) Fatigue properties of AZ31 FSSW coupons were stable under the cyclic force of 1 kN, and the fatigue life of coupons at 1 kN and 3 kN was longer than 1×10^5 cycles and 1×10^4 cycles separately. In addition, all the specimens at higher maximum force had a lower fatigue life than that at lower maximum force.

2) All fatigue failure occurred at the stir zone of FSSW AZ31 magnesium alloy sheet joints, cracks initiated at the stir zone outer edge between the upper sheet and lower sheet, and the failure mode at the lower force level of 1 kN was different from that at higher force level of 3 kN. For the former, the crack propagated along the interface of the heat-affected zone and the thermo-mechanical zone, simultaneously across the direction of force; for the later, the crack propagated along the diameter of stir zone and shear failure occurred finally.

3) There was a tongue-like region at the outer edge of the stir zone between the two AZ31 sheets, and the fatigue crack initiated at the different location of the stirred zone, then propagated along the different directions. When the cycle force was less than the critical resolved shear force of the stirred zone, the crack propagated along the interface of the heat-affected zone and the thermo-mechanical zone, simultaneously across the direction of force; when the cycle force was bigger than the critical resolved shear force of the stirred zone, the crack propagated along the diameter of stir zone and shear failure occurred finally.

References

[1] MORDIKE B L, EBERT T. Magnesium: properties—applications—potential [J]. Materials Science and Engineering A, 2001, 302: 37−45.

[2] AGNEW S R. Wrought magnesium: A 21st century outlook [J]. Journal of Metals, 2004, 56: 20−21.

[3] LUO A A. Magnesium: Current and potential automotive applications [J]. Journal of Metals, 2002, 54: 42−48.

[4] POTZIES C, KAINER K U. Fatigue of magnesium alloys [J]. Advanced Engineering Materials, 2004, 6(5): 281−289.

[5] LOMOLINO S, TOVO R, DOS SANTOS J. On the fatigue behaviour and design curves of friction stir butt-welded Al alloys [J]. International Journal of Fatigue, 2005, 27: 305−316.

[6] MISHRA R S, MA Z Y. Friction stir welding and processing [J]. Materials Science and Engineering R, 2005, 50: 1−78.

[7] TOZAKI Y, UEMATSU Y, TOKAJI K. A newly developed tool without probe for friction stir spot welding and its performance [J]. Journal of Materials Processing Technology, 2010, 210: 844−851.

[8] YIN Y H, IKUTA A, NORTH T H. Microstructural features and mechanical properties of AM60 and AZ31 friction stir spot welds [J]. Materials and Design, 2010, 31: 4764−4776.

[9] YAMAMOTO M, GERLICH A, NORTH T H, SHINOZAKI K. Cracking in the stir zones of Mg-alloy friction stir spot welds [J]. Journal of Materials Science, 2007, 42: 7657−7666.

[10] YANG Q, MIRONOV S, SATO Y S, OKAMOTO K. Material flow during friction stir spot welding [J]. Materials Science and Engineering A, 2010, 527: 4389−4398.

[11] YIN Y H, SUN N, NORTH T H, HU S S. Hook formation and

mechanical properties in AZ31 friction stir spot welds [J]. Journal of Materials Processing Technology, 2010, 210: 2062−2070.

[12] YIN Y H, SUN N, NORTH T H, HU S S. Microstructures and mechanical properties in dissimilar AZ91/AZ31 spot welds [J]. Materials Characterization, 2010, 61: 1018−1028.

[13] LIN Y C, LIU J J, LIN B Y, LIN C M, TSAI H L. Effects of process parameters on strength of Mg alloy AZ61 friction stir spot welds [J]. Materials and Design, 2012, 35: 350−357.

[14] MALLICK P, AGARWAL L. Fatigue of spot friction welded joints of Mg−Mg, Al−Al and Al−Mg alloys [J]. SAE Technical Paper, 2009, 1: 24−27.

[15] JORDON J B, HORSTEMEVER M F, DANIEWICZ S R, BADARINARAYAN H, GRANTHAM J. Fatigue characterization and modeling of friction stir spot welds in magnesium AZ31 alloy [J]. Journal of Engineering Materials Technology, 2010, 132: 1−10.

[16] CHOWDHURY S M, CHEN D L, BHOLE S D, CAO X. Effect of pin tool thread orientation on fatigue strength of friction stir welded AZ31B-H24 Mg butt joints [J]. Procedia Engineering, 2010, 2: 825−833.

[17] AFRIN N, CHEN D L, CAO X, JAHAZI M. Microstructure and tensile properties of friction stir welded AZ31B magnesium alloy [J]. Materials Science and Engineering A, 2008, 472: 179−186.

[18] XIE G M, MA Z Y, GENG L. Effect of microstructural evolution on mechanical properties of friction stir welded ZK60 alloy [J]. Materials Science and Engineering A, 2008, 486: 49−55.

[19] SURESH S. Fatigue of materials, 2nd ed [M]. London: Cambridge University Press, 1998: 63−67.

[20] LAIRD C. The influence of metallurgical structure on the mechanisms fatigue crack propagation [M]//Fatigue Crack Propagation, Special Technical Publication 415. Philadelphia: The American Society for Testing and Materials, 1967: 131−168.

[21] SMITH W F, HASHEMI J. Foundations of materials science and engineering [M]. 4th ed. Beijing: McGraw-Hill Education (Asia) Co. and China Machine Press, 2005: 288−293.

AZ31 镁合金板材搅拌摩擦点焊连接件的疲劳行为

罗天骄，史宝良，段启强，付俊伟，杨院生

中国科学院金属研究所，沈阳 110016

摘　要：利用拉压疲劳实验研究 AZ31 板材搅拌摩擦点焊连接件的疲劳行为。结果表明：AZ31 镁合金板材搅拌摩擦点焊连接件的疲劳失效均发生在搅拌区，疲劳裂纹均起源于搅拌区外侧边缘，位于上下板之间。当循环加载等于 1 kN 时，疲劳裂纹沿着热影响区和热机械区界面且垂直载荷的方向扩展；而当循环载荷等于 3 kN 时，疲劳裂纹则沿着搅拌区直径方向扩展，并最终发生剪切断裂。另外，断口横截面显微分析显示，在 AZ31 板间搅拌区外侧存在一个“舌状区”，“舌状区”的方向是沿搅拌区向外，疲劳裂纹均起源于“舌状区”。

关键词：AZ31 镁合金板材；搅拌摩擦点焊；疲劳；疲劳失效；疲劳裂纹

(Edited by Chao WANG)